Journal of Constructional Steel Research 192 (2022) 107229

Contents lists available at ScienceDirect

Journal of Constructional Steel Research

journal homepage: www.elsevier.com/locate/jcsr

Experimental behavior of circular composite columns with different weld arrangements

Said Boulaares [a,b,*], Djamel Boutagouga [a,b], Abdelkader Houam [a]

[a] Civil Engineering department, Larbi Tebessi University, Tebessa, Algeria
[b] Laboratoire de Génie Civil Appliquée, Larbi Tebessi University, Tebessa, Algeria

ARTICLE INFO

Keywords:
Lateral welds
Longitudinal welds
Concrete-filled
Waste metal plates
Composite columns
Load bearing capacity

ABSTRACT

Eighteen (18) circular short composite columns including 9 concrete-filled steel columns and 9 concrete-filled stainless steel columns, were experimentally studied in this paper. All composite columns have the same dimensions: D= 160 *mm*, H= 300 *mm* and t= 2 *mm*. The objective of this study is to shed light on the effect of the number and arrangement of lateral and longitudinal welds on the resistance and behavior of concrete-filled composite columns. Based on the results obtained, it was confirmed that weld joints have slight effect on the bearing capacity and instability modes of the studied composite columns. Lateral and longitudinal welds were very successful in conveying compression and bending efforts. The experimentally measured load-bearing capacities of the composite columns were compared to those predicted by Eurocode 4, AISC 360–16 and the equation proposed by Giakoumelis and Lam. All the results predicted by the AISC 360–16 code showed a good concordance with the experimental test results. However, the predictions calculated by the EC4 and the equation proposed by Giakoumelis and Lam were not conservative. This investigation shows that the use of lateral and longitudinal welds in composite columns applications would result in a reliable and economical design. This encourages designers to build their confidence in the use of this type of waste metal plates as structural components of locally produced materials.

1. Introduction

Concrete-filled steel tubular (CFST) columns have been widely used in large buildings and bridges [1–3] due to their excellent structural performance characteristics. By combining the beneficial characteristics of steel and concrete, economical and high-performance designs can be achieved. Composite columns offer high strength, high ductility, high rigidity and high fire resistance [3–5]. In addition, steel tubes serve as a permanent formwork for concrete which, effectively reduces construction time and costs [6,7].

In recent years, concerns about environment protection have been rapidly increased in various countries; therefore, researchers in the field of construction and civil engineering have motivated for the reuse of waste material of factories and constructions. Among these waste materials are steel and stainless steel sheet plates. Using these waste materials in civil engineering can help preserve the environment and reduces construction costs. We have thus, developed the idea that the offcuts of steel and stainless steel sheets welded together can form a hollow column. The mechanical behavior of CFST composite columns has attracted the attention of many researchers and have been the subject of numerous studies in different countries. For instance, Sakino et al. [8] explained the underlying mechanisms for developing circumferential tensile stress in the steel tube. In the initial stages of loading circular columns subjected to axial load, since Poisson ratio of concrete is lower than that of steel, the steel tube wall tends to separate from the concrete core. As the load increases, the longitudinal and lateral strains increase until the concrete transverse deformation catches up with that of the steel tube. When the load is further increased, a circumferential tensile stress expand in the steel tube, and the concrete core is subjected to a tri-axial stress state. Giakoumelis and Lam [1] studied the effect of the concrete compressive strength, circular wall thickness and square steel tubes on the concrete-filled steel tubes behavior. Although, there are a few studies that are related to longitudinal welding in composite columns. Ekmekyapar [4], experimentally studied 18 composite columns to evaluate the performance of lateral and longitudinal welded columns. The studied parameters are the ratio L/D (short, medium and long columns), the ratio D/t, and the lateral welding position. Guo et al [9] performed an experimental work on longitudinally welded box

* Corresponding author at: Civil Engineering department, Larbi Tebessi University, Tebessa, Algeria.
E-mail address: said.boulaares@univ-tebessa.dz (S. Boulaares).

https://doi.org/10.1016/j.jcsr.2022.107229
Received 30 September 2021; Received in revised form 26 February 2022; Accepted 2 March 2022
Available online 10 March 2022

sections (square and rectangular) filled with concrete. Chitawadagi [10] studied the axial strength of circular concrete-filled seam welded steel tube columns. Ferhoune [11] studied rectangular sections made of cold-formed steel welded tube subjected to eccentric loading. These studies, show that welding has the potential to be used in the construction of concrete-filled composite columns.

The present work, aims to make a contribution to the understanding of the effect of weld joints on the behavior of short concrete-filled thin hollow circular tubes welded laterally and longitudinally under axial compression while investigating the influence of the number and arrangement of welds, and the type of steel (steel and stainless steel). A total of 18 composite columns comprising 9 steel columns, and 9 stainless steel columns, with different lateral and longitudinal welds locations, were tested. The bearing capacity of the studied composite columns were compared to the values predicted by Eurocode 4 [12], AISC 360–16 revised 2019 [13] and the equation proposed by Giakoumelis and Lam [1]. The obtained experimental results were analyzed and discussed with particular attention to short CFST composite columns behavior in terms of strength and ductility compared to theoretical results.

2. Experimental program

2.1. Specimens

In this work, the structural hollow profiles are made of mild steel and stainless steel sheet plates S265 and S235 respectively. The steel sheets are supplied from the wastes of steel plates produced in the SIDER EL HADJAR Annaba steel complex in Algeria. The investigated composite columns are subdivided into three groups. The first group comprises three longitudinally welded columns by: one, two and three weld joints. They are designated here by: PS-1V-0H, PS-2V-0H and PS-3V-0H respectively. All this three columns contain no transverse (lateral) welds. In the second group, three columns are longitudinally welded by: one, two and three continuous weld joints in addition to a single lateral weld joint. They are designated here by: PS-1V-1H, PS-2V-1H and PS-3V-1H respectively. The third group consists of three longitudinally welded columns by: one, two and three side weld joints with a single lateral weld joint, Fig. 1. They are designated here by: PSD-1V-1H, PSD-2V-1H and PSD-3V-1H respectively. Each one of these three groups is applicable for steel and stainless steel composite columns, resulting in (18) short composite columns, including 9 steel columns and 9 stainless steel columns. All composite columns have the same dimensions: $D=$ 160 mm, $H=$ 300 mm and $t=$ 2 mm, with: D is the outer diameter of the circular tube, t is the thickness of the tube wall, and H is the height of the composite column.

We used the Complete Joint Penetration (CJP) weld type using Shielded Metal Arc Welding (SMAW) to fabricate the circular tubes. The materials and the processes used in structural welding are governed by the American Welding Society (AWS) Specification. We have followed the manufacturing processes of cold-formed steel circular tubes that can be resumed in the following six steps:

- Cut the steel into sheets of the required dimensions.
- Shaping them in a circular shape using forming rollers.
- Surfacing the sheets edges so as to remove the cut defects.
- Cleaning the sheet plates to remove dust.
- Positioning and centering the plates correctly in order to avoid any shift at the welding time.
- Weld the circular shape to form a hollow circular section.

For the columns with a lateral weld joint, the tubes were assembled in two stages in order to avoid welds intersection while assembling the cold-formed steel circular tubes. The first stage consists of executing all longitudinal welds apart. This stage results with an upper half tube and a lower half tube. In the second stage, the resulted upper and lower half tubes are assembled by applying the lateral weld joint to provide the whole circular tube. Finally, weld residues and dust on the inner surface of the tubes were cleaned to improve the interaction between steel and concrete. After cast and hardening of concrete, the upper and lower faces of the composite columns were mechanically treated to eliminate any surface irregularities and ensure that steel and concrete were loaded simultaneously during the test. The main parameters studied are the number and arrangement (lateral and longitudinal) of welds, and the type of steel (steel and stainless steel). The schematic diagram of the investigated composite columns, is shown in Fig. 1.

The adopted composite columns dimensions are chosen with respect to the Eurocode4 and AISC 360–16 revised 2019 technical specifications. These specifications are mainly used to decide on the concrete strength, amount of steel and the thickness of the steel plate, as shown in Table 1. (See Table 2.)

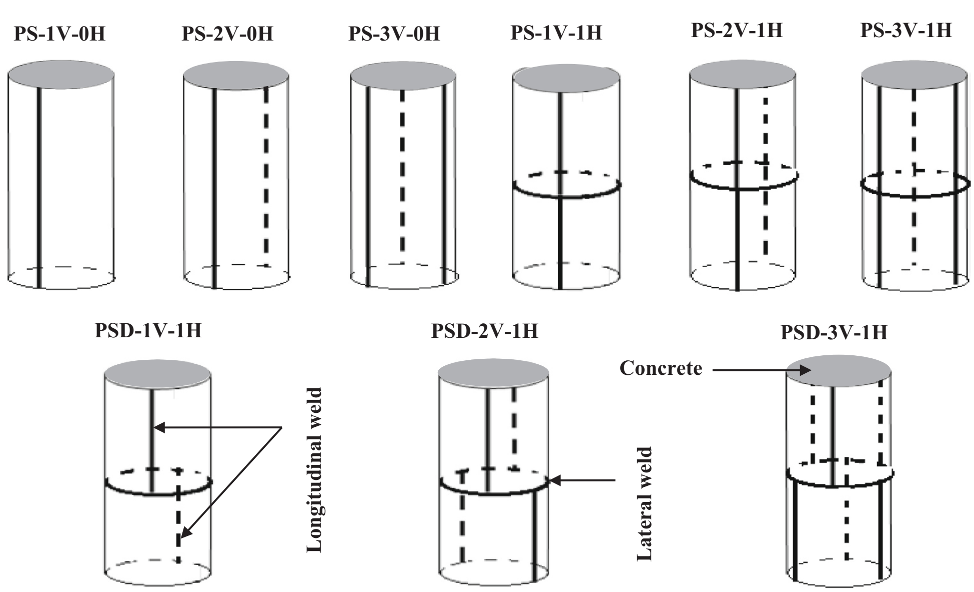

Fig. 1. Schematic diagrams of composite columns with different arrangements of welds.

Table 1
Restrictions specified in EC4 and AISC 360–16-R19 for circular composite columns.

Section	Limitation	Eurocode4	Code limit values			AISC 360–16. R19	Code limit values		
			Steel	Stainles steel	verification		Steel	Stainless steel	verification
Circular	Maximum D/t	$\frac{D}{t} \leq 90 \times \frac{235}{\mathrm{f_y}}$	80	90	✓	$\frac{D}{t} \leq 0.31 \times \left(\frac{\mathrm{E_s}}{\mathrm{f_y}}\right)$	234	264	✓
	Strength of concrete (MPa)	$20 \leq f_c \leq 50$	25		✓	$21 \leq f_c \leq 69$	25		✓
	Yield strength of steel (MPa)	$235 \leq f_y \leq 460$	265	235	✓	$f_y \leq 525$	265	235	✓
	Amount of steel	$0.2 \leq \frac{As \times f_y}{N_{Pl,Rd}} \leq 0.9$	0,4	0,3	✓	$As/Ag \geq 0.01$	0,05		✓

Table 2
Geometric and material properties of composite columns.

Materials	Specimens	D (mm)	L (mm)	t (mm)	D/t	f_y (Mpa)	f_c (Mpa)	As (mm^2)	Ac (mm^2)
	PS-1V-0H	161	298		78			1028	19,320
	PS-2V-0H	160	300		78			1022	19,074
	PS-3V-0H	161	296		78			1028	19,320
	PS-1V-1H	158	294		77			1009	18,588
Steel	PS-2V-1H	157	294	2,06	76	265	25	1002	18,347
	PS-3V-1H	160	295		78			1022	19,074
	PSD-1V-1H	160	296		78			1022	19,074
	PSD-2V-1H	161	297		78			1028	19,320
	PSD-3V-1H	160	294		78			1022	19,074
	PS-1V-0H	161	299		79			1013	19,335
	PS-2V-0H	160	300		79			1007	19,089
	PS-3V-0H	160	303		79			1007	19,089
	PS-1V-1H	160	298		79			1007	19,089
Stainless steel	PS-2V-1H	159	298	2,03	78	235	25	1001	18,845
	PS-3V-1H	158	298		78			994	18,603
	PSD-1V-1H	160	298		79			1007	19,089
	PSD-2V-1H	159	298		78			1001	18,845
	PSD-3V-1H	160	295		79			1007	19,089

2.2. Material properties

The C25/30 concrete class that corresponds to the desired compressive strengths of 25 *MPa* is adopted. The concrete mixture was formulated by using the DREUX-GORISSE method [14]. In order to avoid the disparity of concrete compressive strength, all the specimens were cast vertically in three layers from the same concrete mixture. Each layer was compacted by a concrete vibrator to achieve a more compact and homogeneous concrete over the entire column height. All specimens were stored in a suitable location for the curing at ambient temperature for a period of 28 days. In order to preserve moisture in the specimens, we covered the specimens with tight-fitting plastic lids. The characteristic compressive strength of concrete is 24,441 *MPa* in average measured by 16×32 concrete cylinder at 28 days. The filling concrete formulation is shown in Table. 3. During the concrete cast of specimens, two concrete cylinders were cast from the concrete mixture. These concrete cylinders were tested for compressive strength on the same day of the experimental tests of the composite columns. The compressive strength of the tested cylinders are shown in the Table. 4.

2.3. Test setup

A concentrated monotonic load is applied at the top cross section of the composite columns, as shown in Fig. 2. The axial load is applied using a CONTROLS 2000 kN universal testing machine. Two rigid steel plates of 20 *mm* thickness were used as base plates during the test. One of theme was placed between the composite column and the hydraulic jack in order to distribute the applied load on the whole transverse section. The second one was placed under the composite column to serve as a rigid base. The test was carried out in accordance with Eurocode 4 [12].

Table 3
Mixture of the concrete used to fill hollow columns.

Compositions	Quantity (kg/m^3)
Cement	350
Sand	630,94
Gravel 3/8	263,11
Gravel 8/15	708,12
Water	182

Table 4
Experimentally measured compressive strength.

N°	Compressive strength f_{c28} (*MPa*)	Average f_{c28} (*MPa*)
E1	24.98	25,04
E2	25.11	

All composite columns were centered in the test machine to avoid eccentricity effects. The loading speed is controlled in displacement with a rate of 0.20 *mm*/min and the applied load was increased monotonically up to the failure. One comparator was used to measure the longitudinal displacement, while two other comparators were used to measure the lateral displacements of specimens.

The ultimate load (N_{exp}), ultimate displacement (Δ_{exp}) and failure modes of each tested specimen are the main obtained results from the carried out experimental tests.

3. Comparison of bearing capacity according to design codes

3.1. Eurocode 4

In the Eurocode design code, partial safety factors are applied to material properties. The Eurocode uses partial safety factors to reduce steel yield stress and concrete compressive strength.

The axial load capacity of circular concrete-filled steel columns ac-

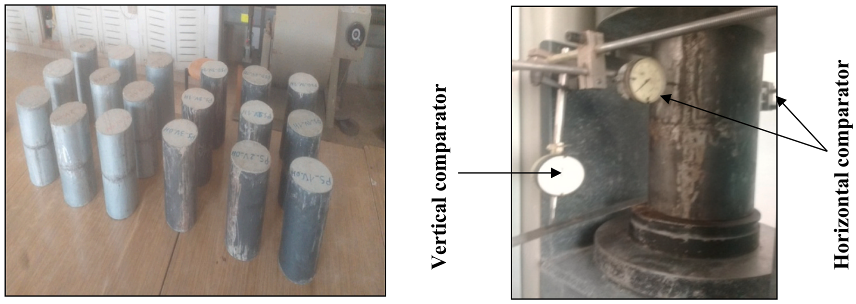

Fig. 2. Pre-tests of composite columns.

cording to the Eurocode 4 is given by the following equations:

$$N_{EC4} = \left(1 + \eta_C \frac{t}{D} \frac{f_y}{f_c}\right) f_c\, A_c + \eta_a f_y A_s \tag{1}$$

$$\eta_c = 4,9 - 18,5\,\lambda + 17\,\lambda^2\ \eta_c \geq 0 \tag{2}$$

$$\eta_c = 0,25\,(3 + 2\lambda)\ \eta_c \leq 1\ \lambda = \left(\frac{N_{PL,R}}{N_{cr}}\right)^{\frac{1}{2}} \leq 0,5 \tag{3}$$

where, N_{cr} is the Euler critical load, given by:

$$N_{cr} = \frac{\pi^2 (EI)_e}{l^2} \tag{4}$$

$$(EI)_e = A_s E_s + 0,6 E_{cm} A_c \tag{5}$$

$N_{PL,R}$ is the plastic resistance of the composite section, given by:

$$N_{PL,R} = f_y A_s + f_c A_c \tag{6}$$

In the above equation (Eq.1 - Eq.6): ηc is the confinement coefficient of concrete, ηa is the confinement coefficient of the steel tube, λ is the relative slenderness, *l* is the buckling length of the composite columns, E_{cm} is the secant modulus of elasticity of concrete and $(EI)_e$ is the effective flexural rigidity, A_a and A_c are the area of steel and concrete respectively, and f_y and f_c are the strength of steel and concrete respectively.

For circular cross-sections with a relative slenderness of 0.2–0.5, the axial load capacity of composite columns can be calculated using the following equation:

$$N_{EC4} = \left(1 + 4,9 \frac{t}{D} \frac{f_y}{f_c}\right) f_c A_c + 0,75\, f_y A_s \tag{7}$$

3.2. AISC 360–16 revised 2019

The AISC 360–16.R19 technical specifications provides an approach for predicting the compressive strength of Concrete-filled steel tube (CFST) columns within the specified limitations presented in Table. 1. The compressive strength of CFST is determined in accordance with the CFST section classification for local buckling, in which $\lambda_P = 0.15\, E_s/f_y$ for a circular section. For a compact section, the compressive strength of the CFST section (P_{no}) is equal to the plastic strength of section (P_P) as follows:

$$P_{no} = P_P = A_s f_y + 0,95\, A_c f_c \tag{8}$$

3.3. Compressive strength by Giakoumelis and Lam [1]

A modification for the ACI (American Concrete Institute) equation was proposed by Giakoumelis and Lam [1]. A coefficient is proposed for the equation to consider the effect of concrete confinement on the load-bearing capacity of circular steel tube filled with concrete. A revision of the equation has been proposed as follows:

$$N_{Eq} = 1,3\, A_c f_c + A_s f_y \tag{9}$$

4. Test results and discussions

The compressive strength of the circular steel concrete-filled columns are listed in Table. 5. By comparing the bearing capacity of the examined CFST columns with one longitudinal weld to those of columns with two and three welds, we can conclude that the number of welds does not have a significant effect on the compressive bearing capacity load of CFST columns.

For the case of steel CFST columns, the axial strength loss were less than 10% in most cases. The axial strength goes from 100% for one longitudinal weld to 97.8% and 95.6% for two and three longitudinal welds, respectively. While, for the columns with lateral weld, the axial strength goes from 95.7% to 92.5% and 80.7% for one, two and three longitudinal welds, respectively and from 86.3% to 0.914% and 1.004% for one, two and three longitudinal side weld joints, respectively. However, for the stainless steel CFST columns, a gain of strength is noticed in all specimens. The axial strength attain 124% for the columns with a lateral weld and two longitudinal weld joints.

The experimental test results are compared against those of the design codes and the equation proposed by Giakoumelis and Lam [1]. It can be noticed from the results listed in Table. 5 that EC4 and the equation proposed by Giakoumelis and Lam [1] overestimate the load bearing capacity of the CFST columns compared to the experimental results. The largest difference is estimated at 57% for steel specimens and 51% for stainless steel specimens. Moreover, it is easy to notice the constant ratio between the EC4 results and the Giakoumelis and Lam equation that is 0.891 for steel specimens and 0.921 for stainless steel specimens.

Unlike the EC4 and Giakoumelis and Lam equation, the AISC 360–16-R19 code provides a reasonable estimation of the axial load capacity for most tested CFST columns. The largest difference between test results and AISC 360–16-R19 is about 21.51% for steel specimens and 11.86% for stainless steel specimens.

According to the obtained results, AISC 360–16-R19 design codes may be preferable for CFST columns due to the reason that the AISC 360–16-R19 underestimates the load bearing capacity of CFST columns. It is important to note that according to Figs. 3 and 4, the number and arrangement of welds does not have a significant effect on the compressive strength of CFST composite columns.

The obtained maximum axial displacements of the top transverse section of the steel and stainless steel CFST specimens obtained from the measuring system of the test device at the moment of weld failure are listed in Table. 6. The obtained results show that the CFST columns with lateral and longitudinal weld joints exhibit ductile behavior under axial loading. In addition, in all the tested columns, the observed failure mode was not brittle. A maximum axial displacement of 7,40 *mm* is recorded.

By examining the behavior of the studied steel and stainless steel CFST columns with different numbers and arrangement of lateral and longitudinal welds shown in Figs. 3-5, one can notice that the number of

Table 5
Comparison of experimental test results with design code results.

Materials		Specimens	N_{exp} (KN)	N_{EC4} (KN)	AISC 360–16 (KN)	N_{Eq} (9) (KN)	$\frac{N_{EC4}}{N_{exp}}$	$\frac{N_{AISC}}{N_{exp}}$	$\frac{N_{Eq(9)}}{N_{exp}}$
Steel	S1	PS-1V-0H	738,20	1008	731	900	1,37	0,99	1,22
		PS-2V-0H	721,90	999	724	891	1,38	1,00	1,23
		PS-3V-0H	706,00	1008	731	900	1,43	1,04	1,28
	S2	PS-1V-1H	706,80	980	709	871	1,39	1,00	1,23
		PS-2V-1H	682,50	970	701	862	1,42	1,03	1,26
		PS-3V-1H	595,63	999	724	891	1,68	1,22	1,50
	S3	PSD-1V-1H	636,70	999	724	891	1,57	1,14	1,40
		PSD-2V-1H	675,00	1008	731	900	1,49	1,08	1,33
		PSD-3V-1H	741,40	999	724	891	1,35	0,98	1,20
Stainless steel	S4	PS-1V-0H	624,40	943	697	867	1,51	1,12	1,39
		PS-2V-0H	722,70	934	690	857	1,29	0,95	1,19
		PS-3V-0H	739,80	934	690	857	1,26	0,93	1,16
	S5	PS-1V-1H	635,00	934	690	857	1,47	1,09	1,35
		PS-2V-1H	774,60	925	683	848	1,19	0,88	1,09
		PS-3V-1H	719,40	916	675	838	1,27	0,94	1,17
	S6	PSD-1V-1H	731,20	934	690	857	1,28	0,94	1,17
		PSD-2V-1H	696,50	925	683	848	1,33	0,98	1,22
		PSD-3V-1H	752,40	934	690	857	1,24	0,92	1,14

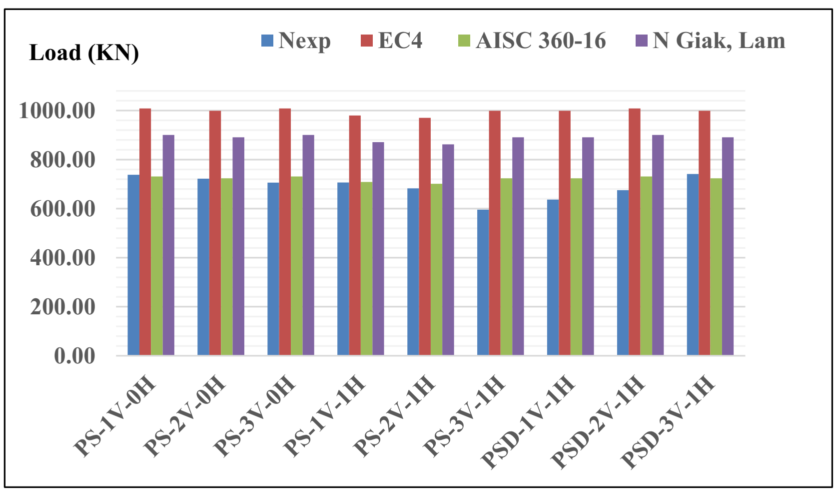

Fig. 3. Comparison of test results axial strength of concrete-filled steel composite columns with those of different design codes.

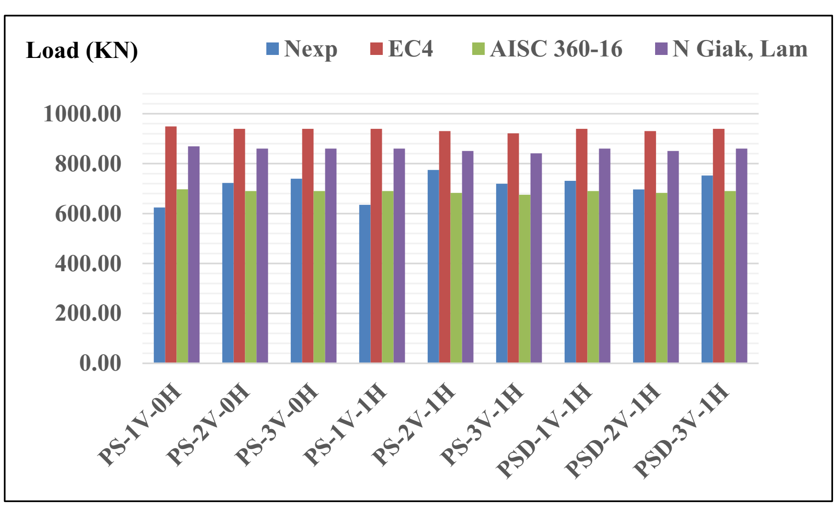

Fig. 4. Comparison of test results axial strength of concrete-filled stainless steel composite columns with those of different design codes.

lateral and longitudinal welds does not have a significant effect on the compressive strength of composite columns. However, the presence of weld joints can influence the overall behavior of CFST columns. It is clear that the number and arrangement of weld joints can significantly influence the ductility of columns. It is easy to notice that, for the steel columns, the ultimate axial displacement decreases as the number of

Table 6
Axial displacements of experimental test results.

Specimen	Axial displacement Δ_{max} (*mm*)	
	steel	stainless steel
PS-1V-0H	5,94	3,1
PS-2V-0H	5,42	5,2
PS-3V-0H	4,58	4,34
PS-1V-1H	4,96	2,32
PS-2V-1H	2,98	5,58
PS-3V-1H	2,17	5,55
PSD-1V-1H	7,4	6,75
PSD-2V-1H	5,96	4,07
PSD-3V-1H	5,13	7,21

longitudinal welds increases. Which means that, the ultimate axial displacement is inversely related to the number of longitudinal welds as shown in Fig. 5. However, the number and arrangement of weld joints has no such effect on the ultimate displacement and overall behavior of the composite stainless steel columns. Note that the measured axial displacements presented in Table. 6 represent the displacements that matches to the maximum axial loads recorded at the moment of weld joint failure.

5. Failure mechanism of CFST columns

The behavior and performance of lateral and longitudinal weld joints is a primary focus of this study. The failure mode of the CFST columns investigated in this work was by fracture of welding in all specimens. During the tests, after a significant axial displacement, we observed cracks of the longitudinal weld joints, then, the failure of concrete is perceived in the local buckling formation area that is triggered after the longitudinal weld joints failure.

Soon after the weld failure, a local outward convex buckling formation is noticed at the longitudinal weld failure area with the gap of steel. We have also noticed that this gap causes a tear that extends to the non-welded part of the composite column, Fig. 6. All CFST columns have collapsed by local buckling and crush of concrete after longitudinal weld joints failure.

The fracture of the weld joint results from the localized tensile stresses in the circumferential direction. This circumferential stress is perpendicular to the longitudinal weld joint, therefore, the failure starts by the longitudinal weld cracks. The failure mode is similar on all tested columns. The failure is located at the lateral and longitudinal welds crossing area, as shown in Fig. 6. However, the most important observation, is that the lateral welds of steel tubes remained intact during the test until the collapse of columns. Even at a high level of deformation in the plastic region, the lateral welds were successful in transmitting compressive and bending actions.

6. Conclusion

In this work, 18 short composite columns were tested till failure under axial compressive centered load. The tested columns consist of concrete-filled steel and stainless steel tubular columns with lateral and longitudinal weld joints. The test results are compared to the axial load capacity calculated according to the Eurocode4, AISC 360–16 revised 2019 and the design method proposed by Giakoumelis and Lam.

The main objective of the study is to investigate the effect of the number and arrangement of weld joints on the CFST composite columns performances.

The following conclusions are drawn from the obtained test results:

1. The examined CFST columns with lateral and longitudinal weld joints exhibits ductile behavior under axial loading.
2. The failure mode of the examined CFST columns was by breakage of longitudinal welding in all specimens.
3. The longitudinal weld joint breakage results from localized tensile stresses in the circumferential direction.
4. The number and arrangement of weld joints can significantly influence the ductility of columns.
5. The number and arrangement of weld joints does not significantly influence the compressive strength of composite columns.
6. Geometric nonlinearity is important in the weld failure development for short columns.
7. AISC 360–16-R19 provides a reasonable estimation of the axial load capacity of CFST columns.
8. EC4 and the equation by Giakoumelis and Lam, overestimates the axial load capacity of CFST columns.
9. The use of side and longitudinal welds in column applications would result in a reliable and cost effective design.

Author statement

As the corresponding author I certify that this manuscript is original and its publication does not infringe any copyright.

As the corresponding author I declare that the manuscript has not been previously published, in whole or in part in any other journal or scientific publishing company. Also the manuscript does not participate

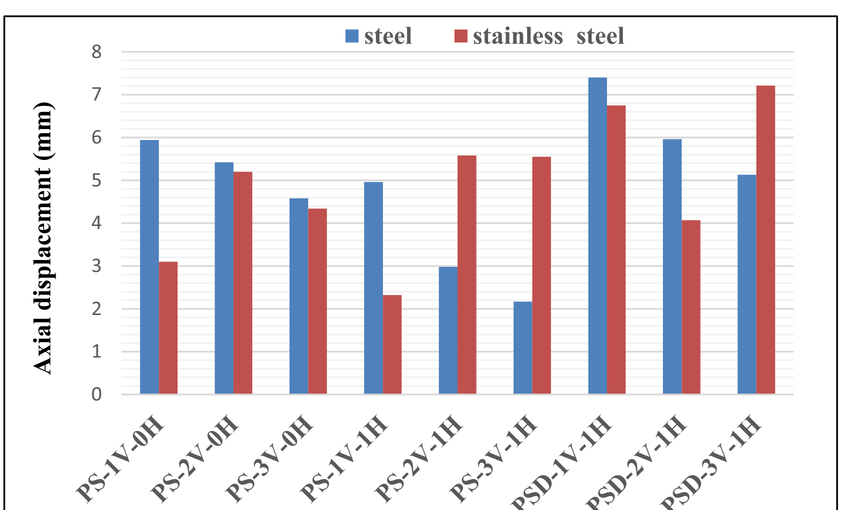

Fig. 5. Influence of the number and arrangements of welds on the axial displacement corresponding to weld failure.

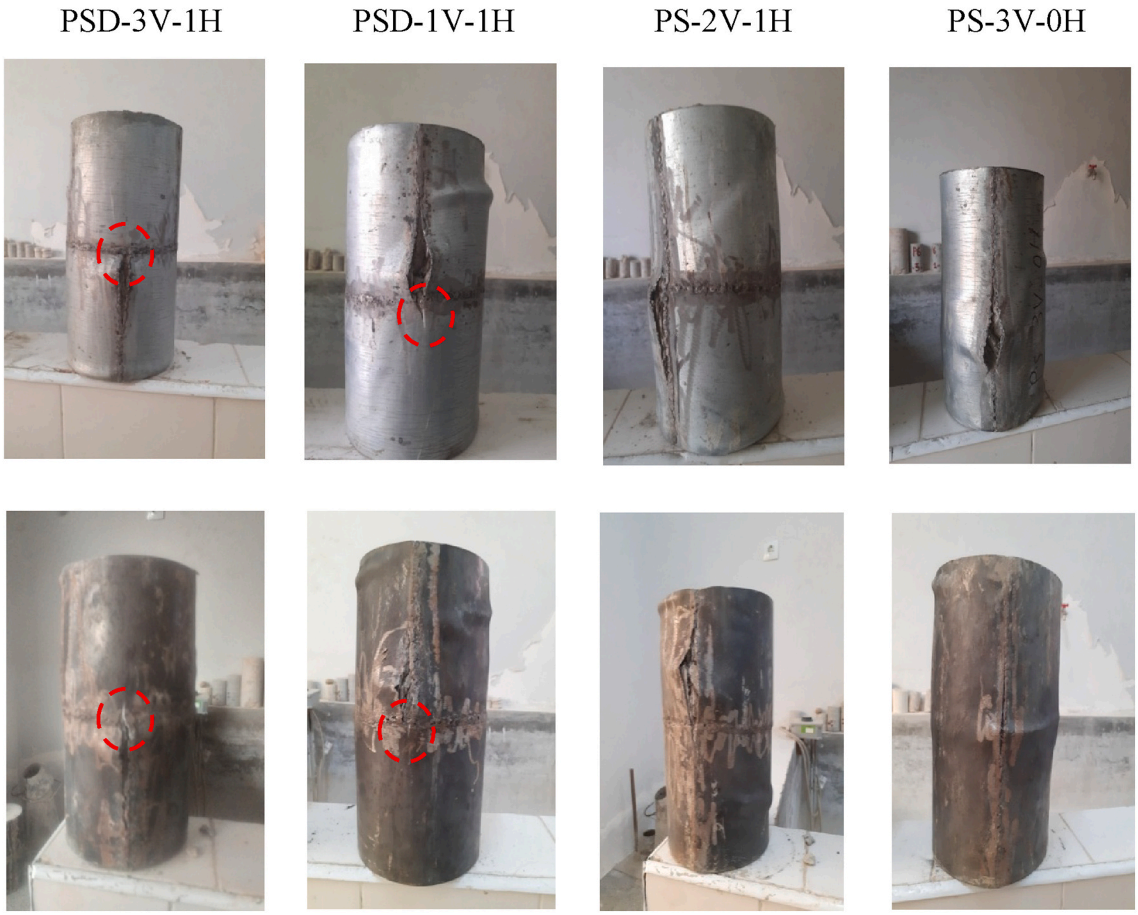

Fig. 6. Failure mode of circular steel and stainless steel composite columns.

in any other publishing process. I also declare there is no conflict of interest.

As the corresponding author I declare that all persons listed hereafter were committed in the creation of the paper and were informed about their participation.

Declaration of Competing Interest

We declare that there is no conflict of interest.

References

[1] G. Giakoumelis, D. Lam, Axial capacity of circular concrete-filled tube columns, J. Constr. Steel Res. 60 (2004) 1049–1068.
[2] N.K. Brown, M.J. Kowalsky, J.M. Nau, Impact of D/t on seismic behavior of reinforced concrete-filled steel tubes, J. Constr. Steel Res. 107 (2015) 111–123.
[3] F. Abed, M. AlHamaydeh, S. Abdalla, Experimental and numerical investigations of the compressive behavior of concrete-filled steel tubes (CFSTs), J. Constr. Steel Res. 80 (2013) 429–439.
[4] T. Ekmekyapar, Experimental performance of concrete-filled welded steel tube columns, J. Constr. Steel Res. 117 (2016) 175–184.
[5] M. Dundu, Compressive strength of circular concrete-filled steel tube columns, Thin-Walled Struct. 56 (2012) 62–70.
[6] E. Ellobody, B. Young, D. Lam, Behavior of normal and high strength concrete-filled compact steel tube circular stub columns, J. Constr. Steel Res. 62 (2006) 706–715.
[7] M.H. Lai, J.C.M. Ho, Confinement effect of ring-confined concrete-filled-steel-tube columns under uni-axial load, Eng. Struct. 67 (2014) 123–141.
[8] K. Sakino, H. Nakahara, S. Morino, I. Nishiyama, Behavior of centrally loaded concrete-filled steel-tube short columns, J. Struct. Eng. 130 (2004) 180–188.
[9] L. Guo, S. Zhang, W.-J. Kim, G. Ranzi, Behavior of square hollow steel tubes and steel tubes filled with concrete, Thin-Walled Struct. 45 (2007) 961–973.
[10] M.V. Chitawadagi, M.C. Narasimhan, S.M. Kulkarni, Axial strength of circular concrete-filled steel tube columns- DOE approach, J. Constr. Steel Res. 66 (2010) 1248–1260.
[11] N. Ferhoune, Experimental behavior of cold-formed steel welded tube filled with concrete made of crushed crystallized slag subjected to eccentric load, Thin-Walled Struct. 80 (2014) 159–166.
[12] EN 1994-1-1 Eurocode 4, Design of Composite Steel and Concrete Structures-Part 1–1: General Rules and Rules for Buildings, CEN, Brussels, 2004.
[13] ANSI/AISC 360–-16 revised 2019, Specifications for Structural Steel Buildings, American Institute of Steel Construction, Chicago, Illinois, USA, 2019.
[14] G. Dreux, J. Festa, New Guide of Concrete and its Constituents, 8th edition, Eyrolles, Paris, France, 1998.